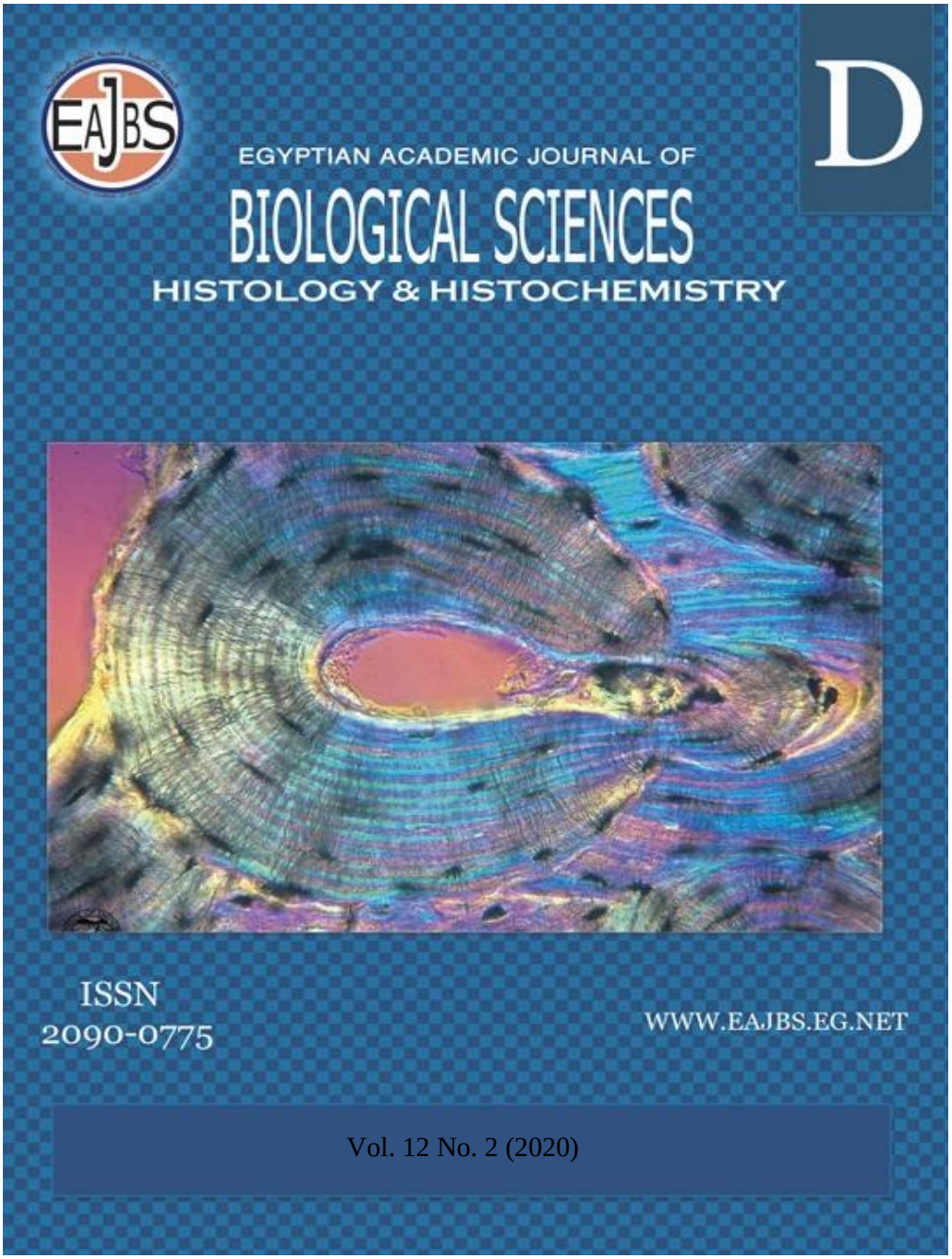

The Journal is an Egyptian journal covering the whole field of general, experimental, systematic and applied entomology. Manuscripts generally should not exceed 30 pages (exceptions are possible, particularly in case of reviews, and should be negotiated in advance with the editors). Papers are considered by referees before acceptance. Authors will receive first editorial decision within 8 weeks from confirmed submission. All contributions are published in English. Authors whose mother tongue is not English are strongly urged to have their manuscripts reviewed linguistically before submission. Papers written in poor English will be returned. It is understood that manuscripts submitted to EAJBS have not been offered to any other journal for prior or simultaneous publication.

http://eajbsd.journals.ekb.eg/

Citation: Egypt. *Acad. J. Biolog. Sci. (D-Histology and histochemistry) Vol.12(2) pp23-44(2020)*

Egypt. Acad. J. Biolog. Sci., 12(2): 23- 44 (2020)

Egyptian Academic Journal of Biological Sciences
D. Histology & Histochemistry
ISSN 2090 – 0775
http://eajbsd.journals.ekb.eg

Effect of Arabic Gum Aqueous Extract on Histological, Ultrastructural, Immunohistochemical and Biochemical Changes on Colistin-Induced Nephropathy in Male Albino Rats

Samah M. Arisha
Zoology Department, Faculty of Science, Menoufia University
E.Mail : **arishasamah@yahoo.com**

ARTICLE INFO
Article History
Received:25/7/2020
Accepted:25/10/2020

***Keywords*:**
Colistin-nephrotoxicity, Arabic gum, Histological& Ultrastructural, Immunohistochemical,

ABSTRACT

Although colistin is an old antibiotic used in the treatment of Gram-negative infections, its usage is associated with nephrotoxicity. Arabic gum (AG) is an edible, dried gummy exudate used in the pharmaceutical and traditional treatment and has a protective effect against nephropathy through its antioxidant action. Aim of this study: This study was performed to demonstrate the role of the Arabic gum aqueous extract (AGAE) in repairing nephrotoxicity induced by colistin. Materials and methods: Forty adult male albino rats were divided equally into four groups. Group 1: Animals of this group served as control ones. Group II: Animals were treated with AGAE only 3 times a week for 8 weeks. Group III: Animals were subcutaneously injected with colistin accumulative dose 84 mg/kg (14mg/kg of body weight in 6 doses one every 2 hours). Group IV: Animals were treated with the accumulative dose of colistin and on the next day they received the AGAE three times a week for 8 weeks. At the end of each experiment, animals were sacrificed and the two kidneys were removed out and prepared for the histological and ultrastructural examination. Sera of animals were collected to determine urea, creatinine, malondialdyhide, and superoxide dismutase. Results: The treatment with AGAE efficiency improving colistin nephrotoxicity is evident from disappeared of most histopathological and ultrastructural alternations. Moreover, the immunohistochemical expression of PCNA and Bcl-2severly increased after colistin treatment. While the AGAE-treatment improved the expressions of PCNA and Bcl-2. Also, it is proven that the AGAE retrains the biochemical parameters determined to the normal ranges. Conclusion: AGAE exerts a protective effect against renal toxicity induced by colistin through its antioxidant, anti-inflammatory, and anti-apoptotic actions.

INTRODUCTION

Colistin (polymyxin E) is an antibiotic used in the treatment of life-threatening Gram-negative infections. Moreover, it is an important constituent of the polymyxin class of cationic polypeptide, antibiotic, and it was once suspended because of its toxicity especially nephro and neurotoxicity (Yahav *et al.,* 2012; Li *et al.,* 2006).

A high nephrotoxicity rate in patients receiving colistin was recorded as 40% to 45% (Pogue *et al.,* 2011). Moreover, the entrance process of colistin to the cell is highly toxic independent of cell membrane damage due to its direct luminal contact (Korucu *et al.,* 2019). Dai *et al.* (2014) reported that oxidative stress is the main factor that drives colistin to induce nephrotoxicity. Recent studies indicated that colistin is associated with substantial excess acute kidney injury that is apparent within the first 72 hours of treatment (Miano *et al.*, 2018).

Acacia gum (Arabic gum, AG) is a water-soluble polysaccharide fiber and produced from dried gummy exudates of *Acacia snegal* (Leguminosae) (Lelon *et al*., 2010). It consists of D-galactose units backbone with branched chains of (1–3)-linkedβ -D-galactopyranosyl units containing α - L -arabinofuranosyl, α- L - rhamnopyranosyl, β- D - glucuronopyranosyl, and 4-O-methyl-β-D -glucuronopyranosyl units. Upon ingestion, AG is fermented in the colon by microorganisms to short-chain fatty acids (Phillips, 1998).

Arabic gum has various pharmacological activities as hepatoprotective (Gamal El-din *et al.*, 2003), improve urinary bladder cytotoxicity (Abd-Allah *et al.,* 2009), antioxidant potential and free radical scavenging ability through a potent for superoxide anions (Hooda *et al*., 2012), antidiuretic effect (Faid, 2013) and ameliorate the chronic kidney disease (AL Suleimani *et al.,* 2015). It has been reported that AG could be beneficial to a patient with acute and chronic kidney failure as it prevents disease progression and delays renal replacement therapy by decreases the production of free oxygen radicals (Staples and Wang, 2010; Mahmoud *et al.,* 2011). Rawoof *et al.* (2017) the AG treatment prevents the elevation of serum creatinine, uric acid, blood urea nitrogen, and suppresses the increase in intracellular calcium. In addition, kidney architecture and oxidative stress, induced by cisplatin, were improved after AG treatment (Al Majed *et al.,* 2002). There were many studies performed to evaluate the protective effect of AGAE but only through one or two parameters. So this study aimed to verify the possible ameliorative effect of AGAE against nephrotoxicity induced by colistin in adult male albino rats through pathological, ultrastrctural, immunohistochemical, and biochemical studies.

MATERIALS AND METHODS

Plant Materials:

Arabic gum *(Gum acacia)* is a dietary fibrous heteropolysaccharide that is cultivated in Sudan. The Sudanese Arabic gum, the type that is commonly and ordinal used by Egyptians, was purchased from the local market in Dubai. The dried gum was ground using an electric matrix into a fine powder and kept in a tightly closed container at 4ºC until used. Gum extract (15% w/v the most common traditional used concentration) was freshly prepared before every used by soaking 15g in 100ml of distilled water, settled for 24 hours, and then filtered (Saad *et al.,* 2018). The filtrate was used; each 1ml contains 0.15g of AG, at a dose of 1.2 g/kg/day**.**

Colistin (induction of nephrotoxicity)

Commercially polymyxin E, colistimethate sodium, is known as colistin is white lyophilized powder in a 7ml glass vial, was purchased from Sigma-Aldric (St. Louis, Mo, USA). Each vial of colistimethate sodium contains 1 million international units powder for solution. Colistin subcutaneously injected at a dose of 14mg/kg of body weight as 6 doses one every 2 hours to reach the accumulative dose 84 mg/kg (Sivanesan *et al.,* 2017).

Animals:

Forty adult male albino rats (*Rattus norvegicus*) weighing from 130-150g were obtained from Helwan farm, ministry of health, Cairo, Egypt. Animals were let for acclimation period at least 10 days before any experimental work. Animals were housed in plastic cages under control environment condition (23± 2ºC and a 12hours light/dark) fed on a commercial standard pellet diet (El-Nasr pharmaceutical Chemicals Co., Cairo, Egypt) and allowed free access to tap water. All the experiments were done in compliance with the guide for the care and use of laboratory animals, faculty of Science, Menoufia University, Egypt (Approval No. MUFS/F/HI/7/20) and according to the National Institutes of Health guide for the care and use of laboratory animals (NIH publications No. 8023, received 1978).

Experimental Protocol:

Animals were randomly divided into four groups (10 rats in each). Group I (control group) animals were received distilled water through a gastric tube for the period of the experiment. Group II (AG group) animals were treated with AGAE only 3 times a week for 8 weeks. Group III (colistin group) animals were subcutaneously injected with colistin sulfate (14mg/kg of body weight in 6 doses one dose every 2 hours to reach the accumulative dose 84 mg/kg. Group IV (colistin + AG group) animals were treated with the accumulative dose of colistin and on the next day, they received the AGAE three times per week for 8 weeks.

At the end of each experiment, animals were sacrificed under the effect of diethyl ether anesthesia and two kidneys were removed and prepared to examine by light and electron microscope.

Histological Analysis:

After dissected of animals in each group two kidneys were removed and small pieces of one kidney were fixed in 10% neutral formalin. An ascending series of alcohol was used for the dehydration of the specimens that were cleared in two changes of xylene and embedded in molten paraffin (mp. 50 – 58 ˚C) then section of 5microns thickness was cut using a rotary microtome. Then these sections were stained with Ehrlich's haematoxylin and counterstained with eosin.

Ultrastructure Studies:

For transmission electron microscopic studies small pieces of the kidney (1 mm) from control and treated groups were fixed in buffered glutaraldehyde (glutaradehyde + formaldehyde) followed by post-fixation in 1% osmium tetroxide. The samples were dehydrated in ethanol series (50- 100%) and embedded in epoxy resin capsules. Capsules were put in a 60ºC oven for 48 hours. Once hardened, the blocks were trimmed and the semithin sections (0.5µm) were cut and stained with toluidine blue and examined with a light microscope. The ultrathin sections were cut, at 60-90nm thick, using a LEICA ULTRACUT UCT microtome then collected onto grids. Sections were dried overnight before staining. Grids were stained with urnayl acetate and lead citrate. Finally, the selected areas of the stained grids were examined and photographed for required magnification using the transmission electron microscope model 1400 plus-JSM (JEOL Ltd., Tokyo, Japan) in the electron microscope unite at Faculty of Science, Alexandria University. All chemicals used in histological and ultrastructure analyses were purchased from Sigma-Aldrich Corp (St. Louis, MO USA).

Immunohistochemical Studies:

Immunohistochemical Staining For Detection of Bcl-2 and Antiproliferated for Nuclear Antigen (PCNA):

For immunohistochemistry techniques 1-2micrometer thickness

sections of the kidney tissue were prepared and stained immunohistochemicaly to determine the expression of proliferation cell nuclear antigen (PCNA) and B-cell lymphoma 2 (Bcl-2), using the suitable antibody in each staining time, anti-PCNA anti-Bcl-2 (Hsu *et al.*, 1981).

Biochemical Analysis:

The blood samples were collected from the anterior vena cava into the laboratorial tubes containing heparin. The collected blood samples were centrifuged at 4000 rpm for 20 minutes then serum was separated and stored at -20ºC until used. Kits for measuring serum creatinine and urea were supplied from Biotechnology Company, Egypt. While kit used for demonstrating malondialdehyde (MDA), superoxide dismutase (SOD), and catalase (CAT) were supplied by Bio Diagnostic Co., Egypt.

Statistical Analysis:

Data were obtained from the experiments were presented as means standard deviations (mean ±SD). Statistical analysis was conducted by one-way analysis of variance (ANOVA) using SPSS (version 23; SPSS, Chicago, IL, USA) to determine differences among experimental groups, with a value of $P < 0.005$ being statistically significant and highly significant at $P < 0.0001$.

RESULTS

Light Microscopic Examination:

Control Group:

Examination of semithin sections of the control group revealed that the kidney is encapsulated by fibrous capsule and consists of an outer cortex and inner medulla. The nephron, the structural and functional unit of the kidney are originated in the cortex at the renal corpuscles that extending to the proximal convoluted tubule then the nephron loop (loop of Henle) extends into the medulla and back to the cortex into the distal convoluted tubule. The renal corpuscles formed of Bowman's capsule that lined by double-walled endothelial layers and tuft of fenestrated capillaries called glomerulus. The outer layer of Bowman's capsule is lined by simple squamous epithelium properly referred to as the parietal layer. The internal leaflet of the capsule, the podocyte cell, appeared enveloping the glomerular capillaries known as visceral layer of Bowman's capsule. The space between these two leaflets is the urinary space. The proximal convoluted tubules are lined by cuboidal epithelial cells provided with a brush border. These cells have eosinophilic granular cytoplasm with single spherical nuclei located in the middle to basal part of the cells. Moreover, the distal convoluted tubules have a wider lumen lined with cuboidal epithelial cells that have no brush border. The cytoplasm of these cells is pale contains a rounded nucleus close to the apical part of the cell (Fig. 1a).

Treated Groups:

1-Treatment with Arabic Gum Aqueous Extract (AGAE):

Examination of kidney semithin sections of the animals treated with AGAE revealed no pathological changes and the structure of the renal cortex appeared almost similar to the control group (Fig. 1b).

2-Effect of Colistin Accumulative Dose:

Light microscopic examination of renal cortex of animals treated with colistin revealed a marked distortion of renal cortical architecture. Many glomeruli appeared atrophied and shrunk and the glomerular tuft showed solid appearance due to wrinkle and collapse of their capillaries. The Bowman's capsules appeared distorted with degenerated lining epithelial cells and widening of the urinary space. Both proximal and distal convoluted tubules showed a variable degree of pathological alternations. The change of necrosis associated with pyknosis of tubular epithelial nuclei, retraction, and loss of

continuity, junction complexes, between the tubular epithelium and basal membrane together with the degeneration of tubular epithelium associated with cytoplasmic vacuolization and wrinkled basement membrane. These findings overlap somewhat of acute tubular injury. The lining epithelial cells of both proximal and distal convoluted tubules appeared flattening or atrophied with vacuolated cytoplasm and pyknotic exfoliated nuclei. Moreover, erosion of the brush border of most of proximal convoluted tubules was seen (Fig. 2a & b). Atrophic tubules cannot be identified as proximal or distal ones they are very low height with thickened basement membrane and widen lumen. In addition, hemorrhage between renal tubules (hemorhagic edema) and congested blood vessels with hemolysis blood cells appeared. Formation of hyaline casts, dilation of distal tubules that indicates marked renal nephritis was observed (Fig. 2c &d).

3-Effect of AGAE treatment on nephrotoxicity

Examination of the kidney of rats treated with AGAE after induction of nephrotoxicity by colistin showed an obvious degree of recovery of renal cortex. Both Bowman's capsules and renal tubules revealed normal built up except a few degenerative sings still appeared. In addition to the glomeruli appeared with normal size both proximal and distal convoluted tubules appeared with mostly normal lining and regular lumen except few tubular cells still have vacuolated cytoplasm and irregular membrane (Fig. 3).

Ultrastructure Observations:

Control Group:

Transmission electron examination of ultrathin sections of control animals showed normal architecture of renal cortex. The glomerulus consists of a tuft of specialized capillaries that are placed in urinary space limited by Bowman's capsule. The wall of glomerular capillaries is a three-structure one; consists of an inner layer of endothelial cell, an outer layer of visceral epithelial cells (podocyte), and an intermediate basement membrane (Fig. 4a). These three structures form glomerular filtration barrier. The inner fenestrated endothelium layer is formed of a single layer of flattened cells. The nuclei of these cells are usually located at the axial region of the capillaries and the cytoplasm contains small, round mitochondria, Golgi apparatus, pinocytic vesicles, and multivesicular bodies. The visceral lining of the capsule is composed of large cells called podocyte that have a cell body from which arise several primary processes each one gives rise to numerous secondary (foot) processes or pedicles which give rise to the slit valves (filtration slits). The basement membrane is a fused membrane (fusion of capillary and podocyte basal lamina) bind integrin of both the podocyte and endothelial cell membrane (Fig. 4b&c). In addition to capillary endothelial and podocyte, renal corpuscle also contains masangial cells that are modified smooth muscles cell (have contractile ability) are characterized by an elongated irregular cytoplasmic projection which penetrates into a subendothelial zone of the glomerular basement membrane (Fig. 4d).

The proximal convoluted tubules lined by epithelial cells rest on basal membrane and characterized prominent apical brush border. Their cytoplasm contained euchromatic rounded nuclei with prominent nucleoli surrounded by prominent endocytic and lysosomal compartments, a large number of mitochondria, and the Golgi apparatus that localized close to the nucleus. The apical cytoplasm contains numerous vesicles near the base of microvilli (Fig. 5a). The distal convoluted tubules cells are tall cuboidal epithelial rest on a thin basement membrane contain apical euchromatic rounded nuclei and

long mitochondria oriented vertically among deep enfolding of the basolatteral plasma membrane and had scarce apical microvilli (Fig. 5b).

Treated Groups:

1-Treated with Arabic Gum Aqueous Extract (AGAE)

Examination of ultrathin sections obtained from renal cortex of animals received AGAE showed a non-remarkable difference when compared with control group. The bowman's capsules appeared normal with normal parietal squamous cells resting on a thick basement membrane and the glomeruli appeared in normal size and structure (Fig. 6a&b). Moreover, cells of both proximal and distal convoluted tubules appeared with normal basement membranes, nuclei, mitochondria, and apical borders (Fig. 6c&d).

2-Effect of Treatment with Colistin:

The ultrastructure examination of adrenal cortex of animal administered colistin showed a marked distortion of Bowman's capsules, glomeruli, filtration barrier, and concerning the tubular damage it was varied from one cortical area to another. As well as, damage of filtration barrier, where the area of focal thickening of capillaries basement membranes, was seen. The distorted glomerular capillaries with indistinct endothelial fenestration resting on a thick basement membrane, variation of its thickness were seen (Fig. 7a). Damaged podocyte cells appeared with affected food processes, degenerated mitochondria intended nucleus, and cytoplasmic vacuolization (Fig. 7b). Moreover, the congested blood vessel and the degenerated masangial cell contain rarified cytoplasm with a dark nucleus appeared (Fig. 7c &d).

The lining cells of the proximal convoluted tubules showed many ultrastructural alternations. These cells appeared reduced in height, the brush borders lacking focally and the apical endocytic invagination appeared less. Moreover, the cytoplasm of these cells appeared rarified or vacuolated contained pyknotic nuclei, few numbers of mitochondria that appeared degenerated with partially or completely damage of cristae (Fig. 8a &b). The cells lining distal convoluted tubules appeared atrophied with rudimentary brush border, few numbers of mitochondria, and degenerated cytoplasmic organelles. Some of these cells rest on a thickened basement membrane and have an abnormal nucleus with irregular nuclear envelop and wide perinuclear cisternae and abnormal distribution of chromatin within the rarified cytoplasm were seen (Fig. 8c&d).

3-Aqueous Extract of AG Alleviated the Nephrotoxicity of Colistin:

Ultrathin examination of adrenal cortex of animals treated with AGAE after induction of nephrotoxicity by colistin showed an obvious degree of improvement. The capillary lumen with normal endothelial cells rest on a regular basement membrane with normal fenestration areas was observed. As well as the podocyte appeared with no ultrastructural alternations having normal foot processes (Fig. 9a&b). Lining cells of proximal convoluted tubules appeared to rest on a uniform regular basement membrane and a well-developed brush border. In addition, a normal round euchromatic nucleus, a large number of elongated mitochondria with some distorted one, and no cytoplasmic vacuoles appeared (Fig. 9c). Moreover, the lining cells of distal convoluted tubules appeared nearly normal with few degenerative features. The cytoplasm contains normal euchromatic nucleus, surrounded by round mitochondria, some lysosomes and few cytoplasmic vacuoles (Fig. 9d).

Immunohistochemical Results:

Bcl-2 immunoreaction:

The Bcl-2 oncoprotein was detected in normal and diseased renal

cortex was examined and its antigen was mainly localized in the cytoplasm of positive cells. In normal adrenal cortex sections, the Bcl-2 immunostaining was almost no detectable in the cell of glomeruli and tubules and interstitum of animals treated with AGAE as well as control group (Fig.10a &b). Examination of renal cortex of animals treated with colistin showed more numerous apoptotic cells denoted +ve Bcl-2 immunoreaction when compared with control group. The reaction is mainly localized as brown granules filling the vicinity of cytoplasm of many cells lining the proximal convoluted tubules, paritial cells of glomeruli, and interstitium (Fig.10c). On the other hand, the expression of Bcl-2 immunoreaction appeared in few cells of the proximal convoluted tubule and parietal cells of glomeruli in animals treated with colistin followed by AGAE (Fig.10d).

PCNA Immunoreaction:

Examination of adrenal cortex in control and AG groups showed few numbers of cells with +ve expression of PCNA. The reaction appeared as brown color in the nuclei of glomeruli, tubules, and interstitium of these animals (Fig. 11a &b). In colistin-treated rats, the PCNA expression has appeared in a large number of nuclei when compared with control group (Fig. 11c). The expression of PCNA in animals treated with colistin and AGAE was detectable in few numbers of cells of glomeruli, proximal tubules, and interstitium (Fig. 11d).

Biochemical Results:

Renal Function:

Animals orally administered AGAE only recorded a non-significant difference in the concentrations of urea and creatinine (18.90±1.42 and 0.94±0.06 respectively) when compared with control group (18.91±1.75and 0.84±0.17 respectively). Whereas, there was a highly significant increase in the concentrations of blood urea and creatinine was recorded when animals were treated with colistin (50.43±4.05 and 3.79±0.33 respectively) when compared with control group. While animals treated with AGAE following nephrotoxicity recorded a significant decrease in the concentrations of urea and creatinine (28.23±1.27 and1.57± 0.16 respectively) when compared with colistin group (Figs. 12&13).

Oxidative Stress:

The treatment with the AGAE recorded a non-significant change in the level of lipid peroxidation that represented by MDA level (7.59±0.30) when compared with normal rats (6.95±0.30). As well as, treatment with AGAE did not affect the level of blood superoxide dismutase (SOD) and catalase activities (61.17±1.16 and 39.70±1.15 respectively) when compared with control group (65.00±3.89 and 43.8±2.85 respectively). A highly significant increase in the level of MDA (26.00±3.47) and a highly significant decrease in the SOD and CAT activities (23.00±5.47and12.70±3.65 respectively) were recorded in colistin group when compared with control ones. While animals treated with AGAE following colostin recorded a significant decrease in the level of MDA (11.20±0.37), (Fig. 14), and a significant increase in the activities of SOD and CAT (55.67±2.16 and 37.10±1.15 respectively) when compared with colistin group (Figs. 15&16).

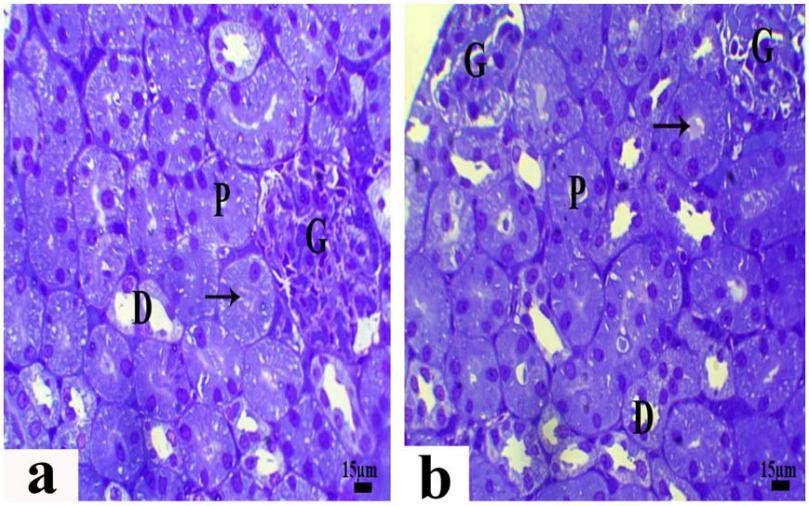

Fig. 1: photomicrograph of semithin sections of renal cortex; (a) of a control rat and (b) of an animal treated with AGAE showing renal corpuscle contains glomeruli (G), proximal convoluted tubules (P), brush border (arrow) and distal convoluted tubules (D), (Toluidine blue, X 400).

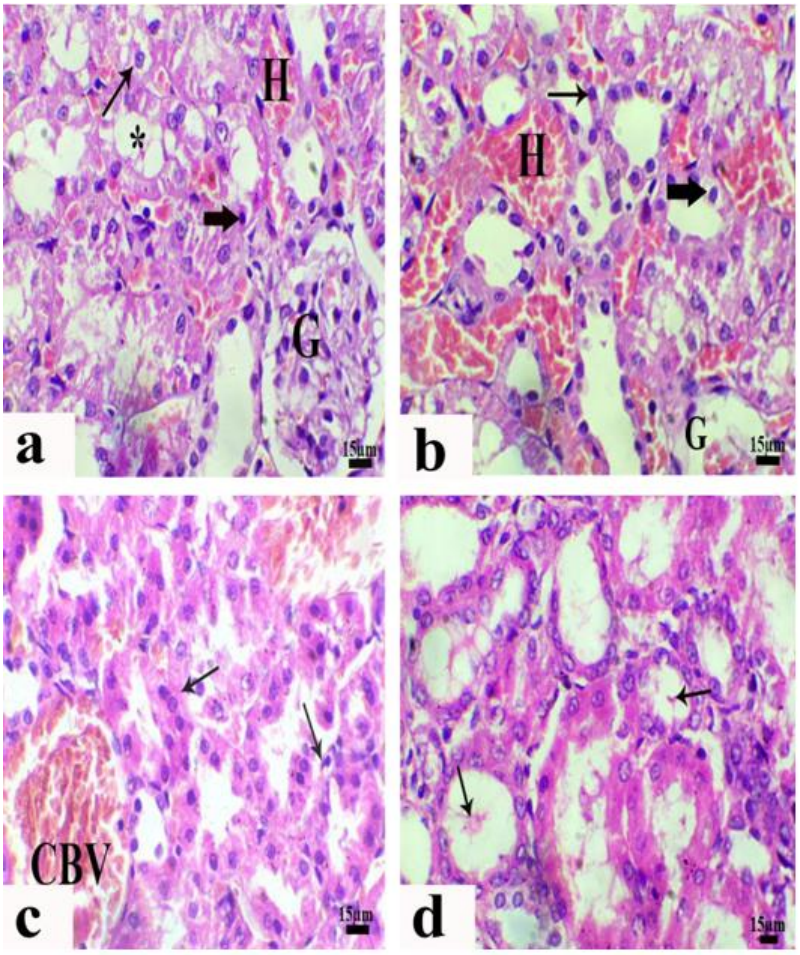

Fig. 2: photomicrograph of sections of renal cortex of animals treated with colistin showing; (a): abnormal glomerulus (G), degenerated tubular epithelium with vacuolated cytoplasm (thin arrow), pyknotic nuclei (thick arrow), protein cast (*) and sever interatubular hemorrhage (H), (b): showing degenerated glomeruli (G), tubular epithelium with pyknotic nuclei (thin arrow), vacuolated cytoplasm (thick arrow) and interatubular hemorrhage (H), (c): showing degenerated convoluted tubules (arrows) and congested blood vessel (CBV), (d): showing degenerated convoluted tubules appeared low height, cannot be identified the proximal or distal one with wide lumen contains protein casts (arrows), (H& E, X 400).

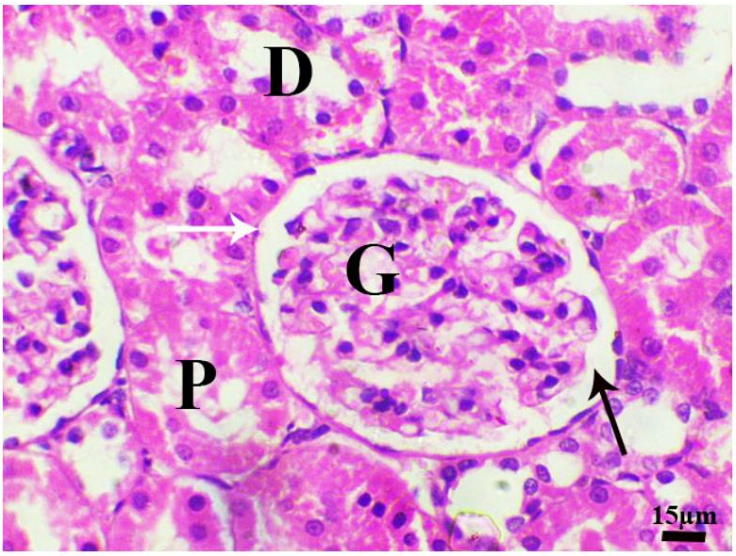

Fig. 3: photomicrograph of a section of renal cortex of an animal treated with colistin and AGAE showing an obvious improvement; nearly normal Bowman's capsule (white arrow), glomerulus (G), urinary space (black arrow), proximal (P) and distal (D) convoluted tubules, (H& E, X 400).

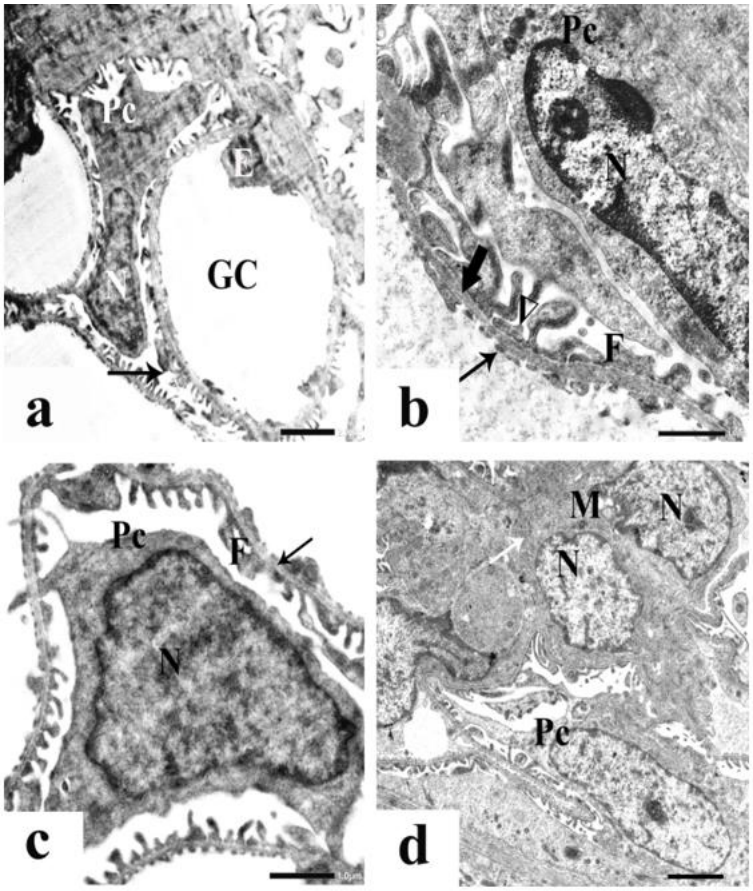

Fig. 4: Electron micrograph of sections of renal cortex of control animals showing; (a): glomerular capillary (GC), endothelial cell (E), podocyte (Pc) with normal euchromatic nucleus (N), and foot processes (arrow), (X 3000). (b): part of glomerular capillary with filtrating barrier has fenestrated endothelial lining (thin arrow) lying on a uniform basement membrane (thick arrow), podocyte (Pc) with nucleus (N), minor processes (F) has filtrating site (Δ) in between, (X 60000). (c): normal podocyte (Pc) with euchrmatic nucleus (N), extending foot process (F) to lie of the basement membrane (arrow), (X 1500). (d): normal podocyte (Pc), masangial cell (M) with euchromatic nucleus (N) and masangial matrix (arrows) (X 3000).

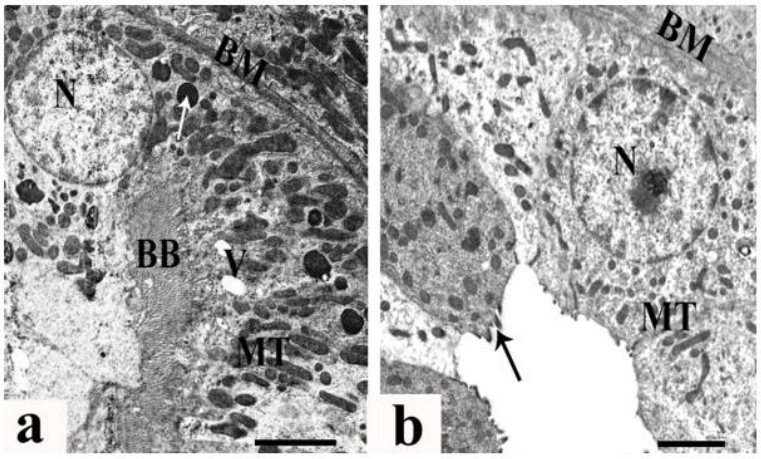

Fig. 5: Electron micrograph of sections of renal cortex of control animals; (a): showing proximal tubular epithelial cell with thin basement membran (BM), euchromatic neuclus (N), elongated mitochonderia(MT), lysosome (arrow), apical vacuoles (V) and brush border (BB), (X 1500). (b): showing proximal tubular epithelial cell with basement membran (BM), euchromatic neuclus (N), elongated mitochonderia (MT) and few apical microvilli (arrow) (X 3000).

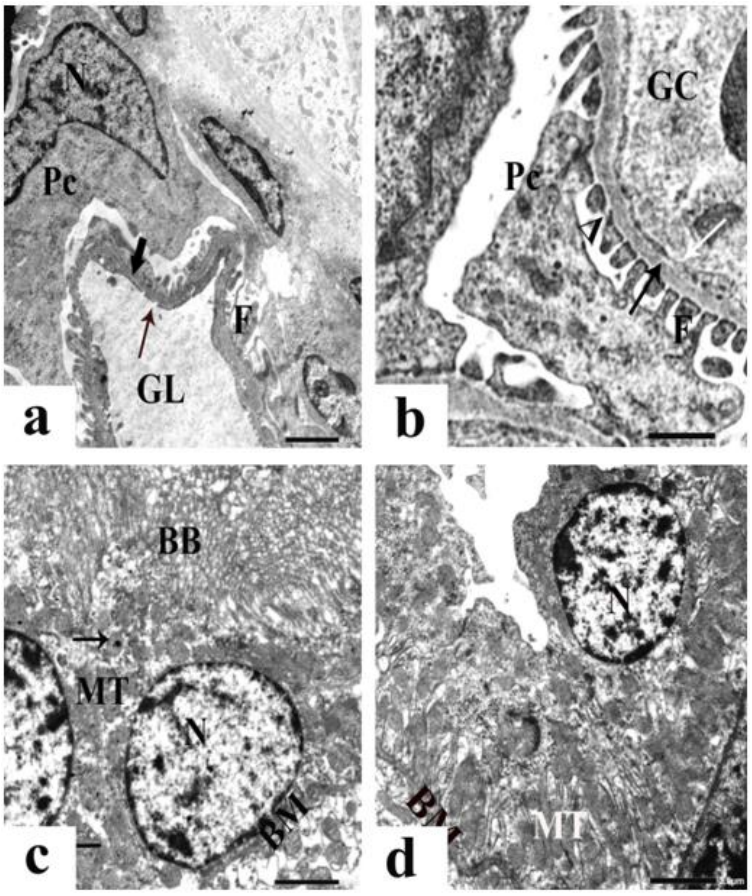

Fig. 6: Electron micrograph of sections of renal cortex of animals treated with AGAE; (a): showing glomerular capillary (GL) with fenesterating endothelial lining (thin arrow), podocyte (Pc) with foot processes (F) lie to the basement membrane (thick arrow), (X 3000). (b): showing normal filtrating barrier, fenesterating endothelial lining (white arrow), basement membrane (black arrow) and minor foot processes (F) of podocyte (Pc) include filtrating site in between (Δ), (X 6000). (c): showing normal proximal convoluted tubular cell rest on thin basement membrane (BM) with euchromatic nucleus (N), large number of mitochondria (MT), endosome (arrow) and brush border (BB), (X 3000). (d): showing distal convoluted tubular cell with thin basement membrane (BM), apical nucleus (N) and elongated mitochondria (MT) (X 3000).

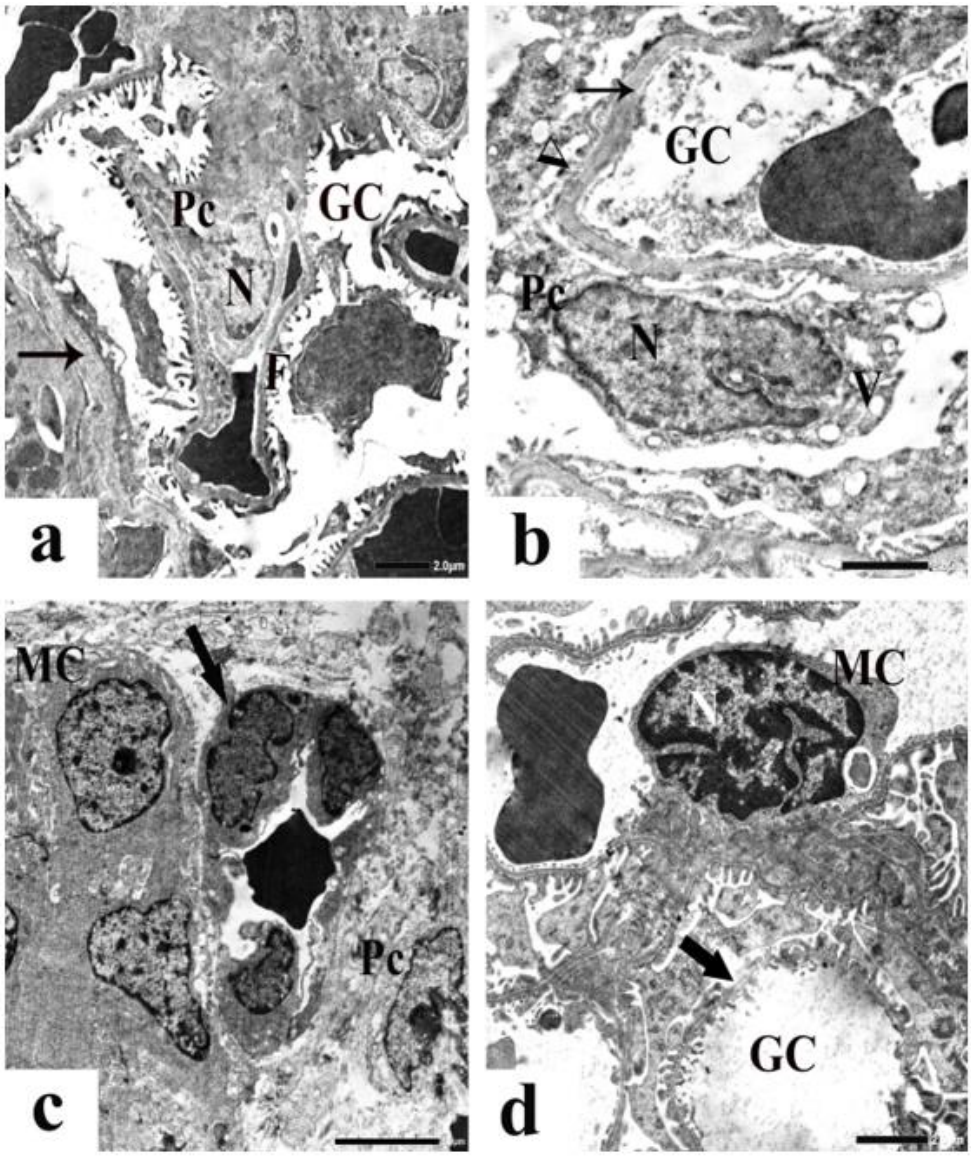

Fig. 7: Electron micrograph of sections of renal cortex of animals treated with colistin showing; (a): abnormal glomerular capillary (GC), with degenerated endothelial lining cell (E), thick basement membrane (arrow), degenerated podocyte (Pc) with nucleus (N) and fragmented foot processes (F), (X 3000). (b): showing degenerated glomerular capillary (GC), thick basement membrane (arrow), degenerated podocyte (Pc) with intended nucleus (N), vacuolated cytoplasm (V) and distorted foot processes (Δ), (X 3000). (c): showing degenerated masangial cell (MC), Podocyte (Pc) and congested blood vessel (arrow), (X 1500). (d): showing degenerated glomerular capillary (GC), filtrating barrier (arrow), masangial cell (MC) contain abnormal nucleus (N) with condensed chromatin material (X 3000).

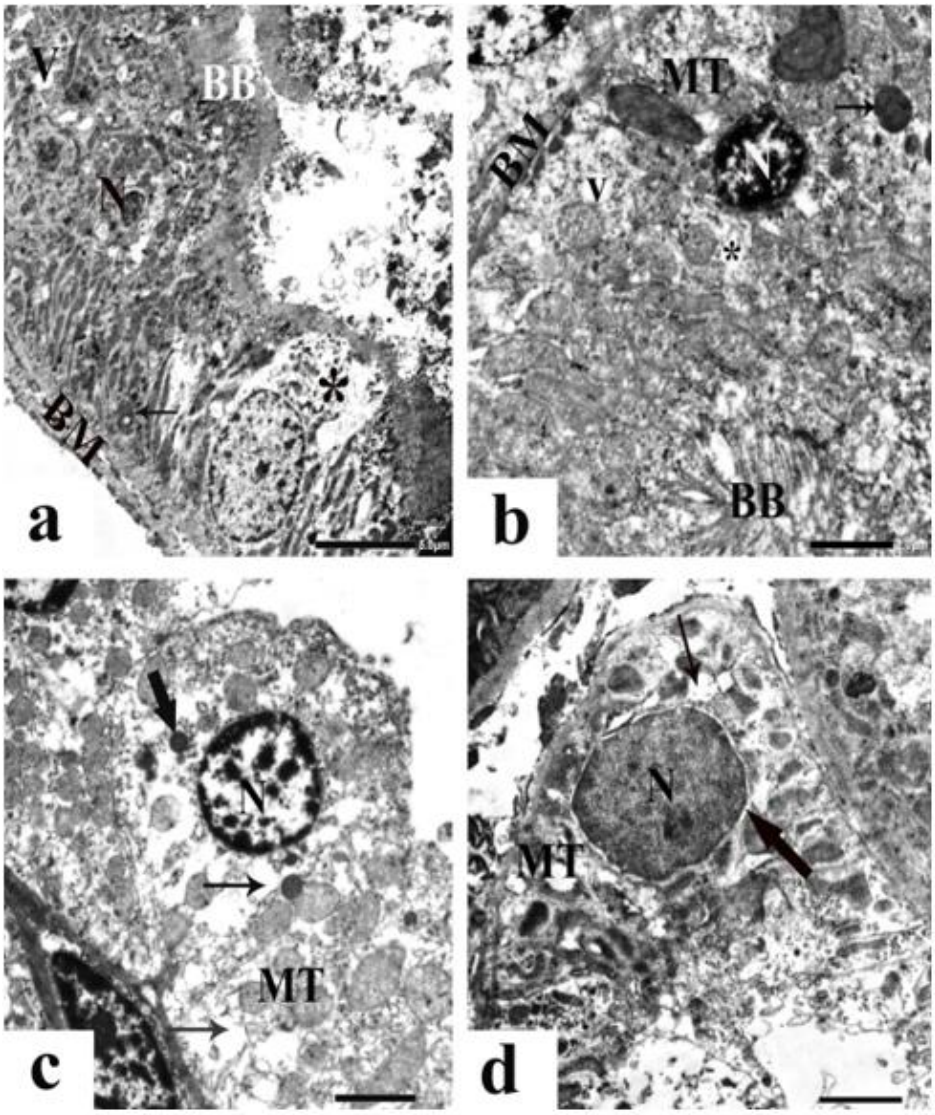

Fig. 8: Electron micrograph of sections of renal cortex of animals treated with colistin showing degeneration of some proximal tubular epithelial cells rest on thick basement membrane (BM) have rarified cytoplasm (*), pyknotic nuclei (N), cytoplasmic vacuole (V), endosomes (arrow) and fragmented brush border (BB) (X 1500). (b): showing degenerated proximal tubular cell with irregular basement membrane (BM), pyknotic nucleus (N), lysosome (arrow), degenerated mitochondria (MT), rarified cytoplasm (*), some vacuoles (V) and fragmented brush border (BB), (X 3000). (c): showing degenerated distal tubular cell with rarified cytoplasm (thin arrow), lysosomes (thick arrow), few number of mitochondria (MT), skunk nucleus (N) with abnormal distribution of chromatin material (X 3000). (d): showing degenerated distal tubular cell withrarified cytoplasm (thin arrow), dark nucleus (N), irregular nuclear envelop and wide perinuclear cisternae (thick arrow) and degenerated mitochondria (MT) (X 3000).

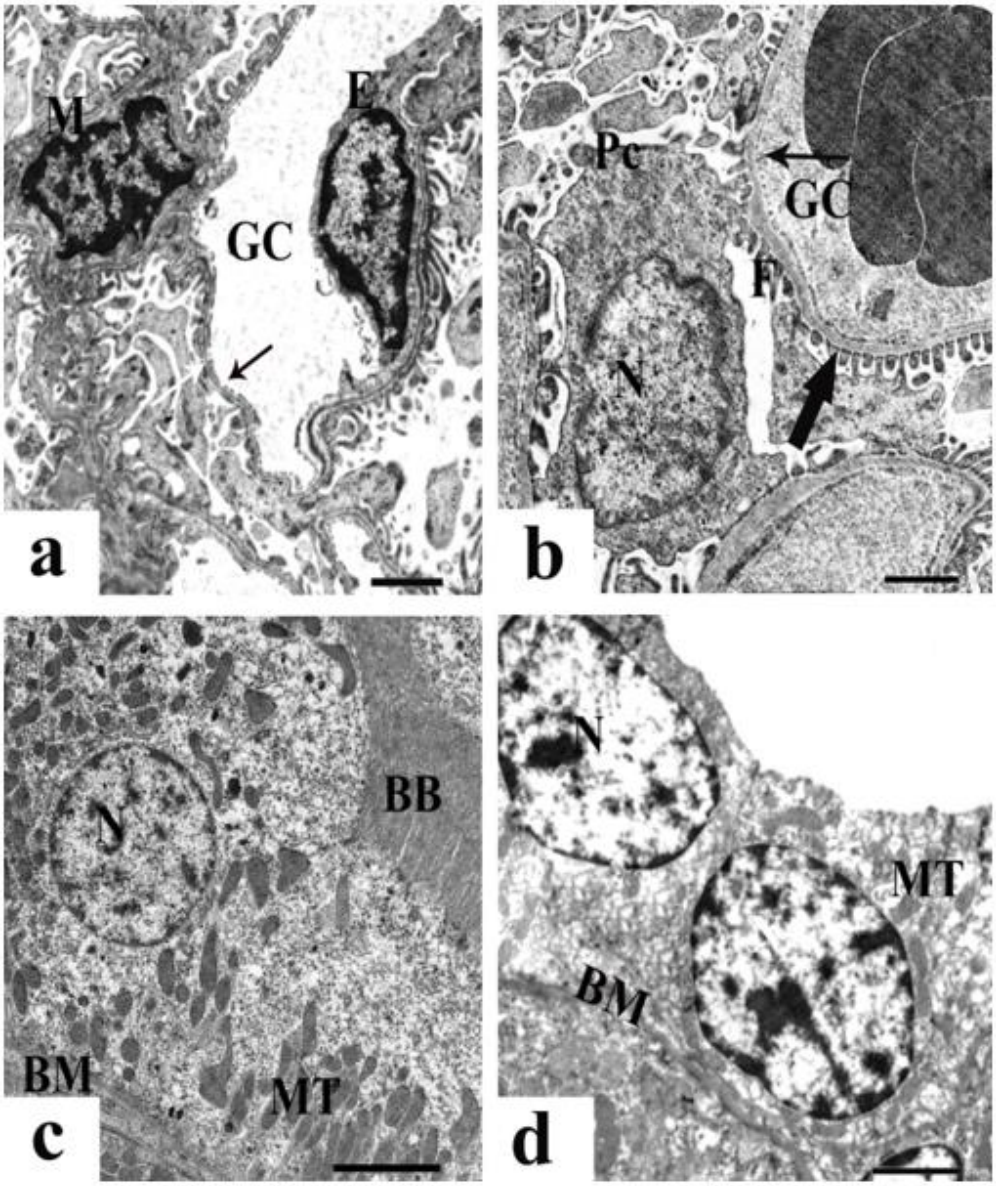

Fig. 9: Electron micrograph of sections of renal cortex of animals treated with colistin and AGAE; (a): showing mostly normal glomerular capillary (GC), endothelial cell (E), fenestrating lining (arrow) and mesangail cell (M), (X 3000). (b): showing glomerular capillary (GC), filtrating barrier with normal fenestrating lining (thin arrows), podocyte (Pc) with normal nucleus (N) and foot process (F) include filtrating site in between (thick arrow), (X 1500). (c): showing proximal tubular cell with normal basement membrane (BM), nucleus (N) and mitochondria (MT) and brush border (BB), (X 3000). (d): showing distal tubular cell with mostly normal basement membrane (BM), nucleus (N) and mitochondria (MT) (X 3000).

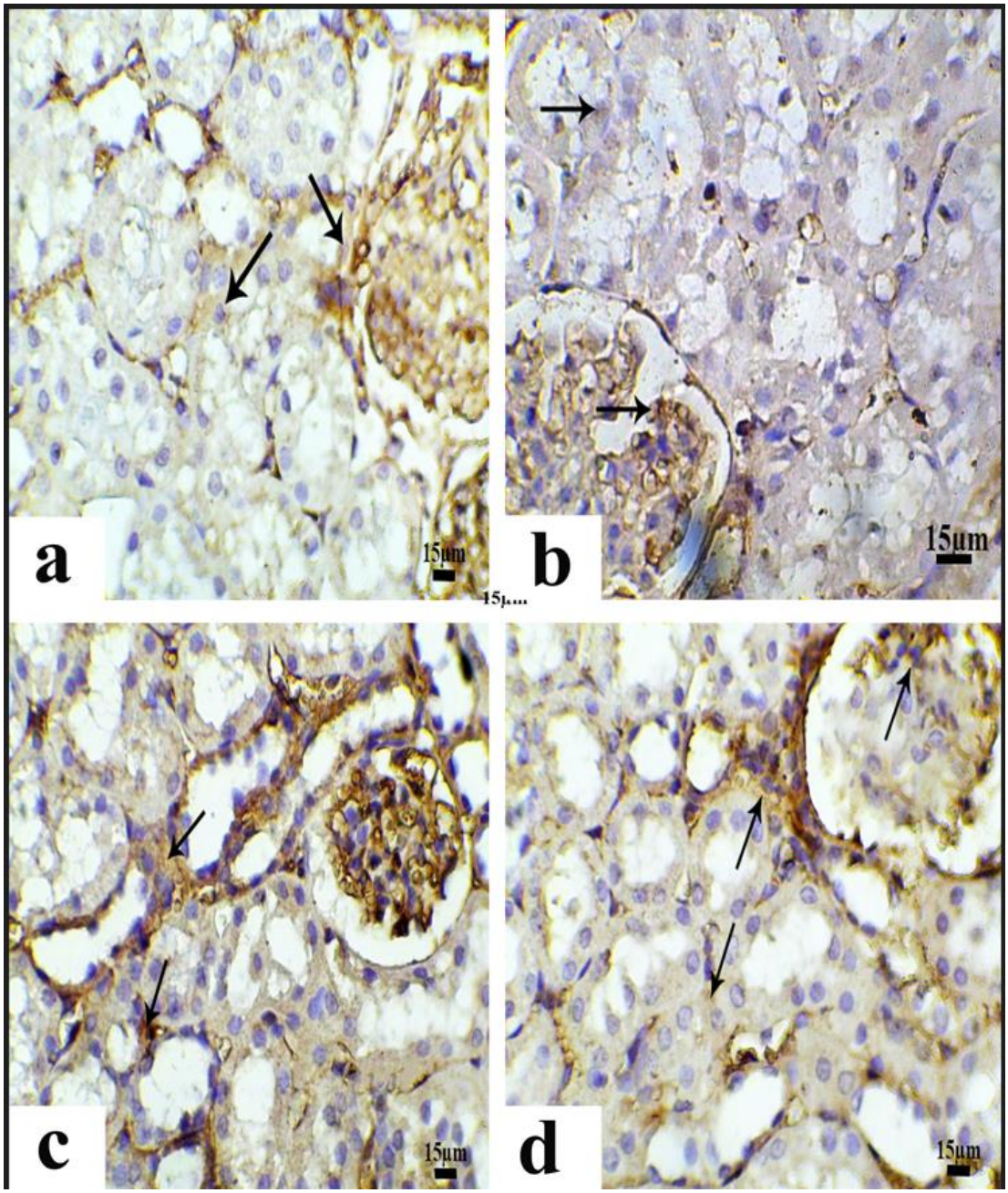

Fig. 10: photomicrograph of sections of renal cortex (a): of a control rat showing Bcl-2 expression appeared in few glomerular, tubular cells and interstitium (arrows), (b): of an animal treated with AGAE showing Bcl-2 expression in few cells of glomerular and tubular epithelium (arrows), (c): of an animal treated with colistin showing positive Bcl-2 expression in the cytoplasm of large number of glomerular and tubular cells (arrows), (d): of an animal treated with colistin followed by AGAE showing few numbers of cells with positive Bcl-2 expression (arrows), (X 400).

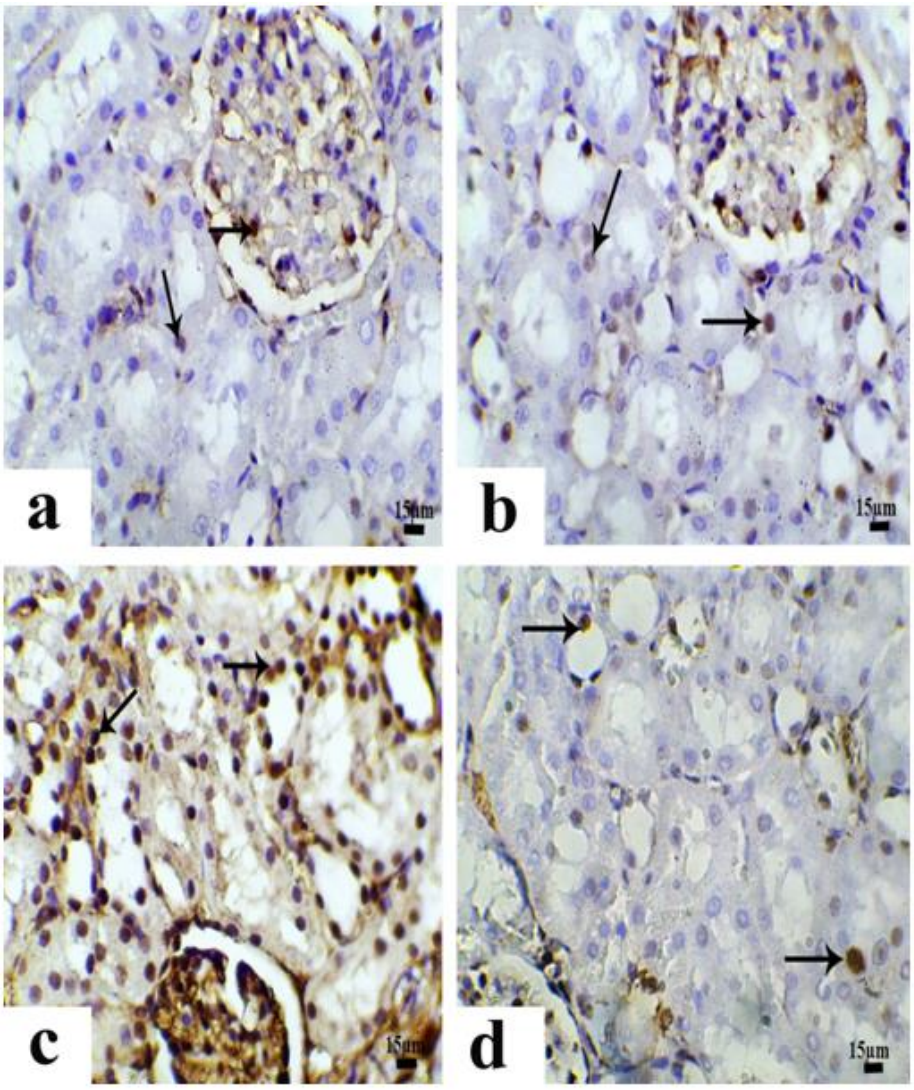

Fig. 11: photomicrograph of sections of renal cortex (a): of control rats showing few numbers of tubular cells with positive PCNA expression (arrows), (b): of an animal treated with AGAE showing PCNA expression in few cells of glomerular and tubular epithelium (arrows), (c): of an animal treated with colistin showing positive PCNA expression in large number of tubular cells and partial cells in glomeruli (arrows). (d): of an animal treated with colistin and AGAE showing positive PCNA expression in few numbers of tubular and glomerular cells (arrows) (X 400).

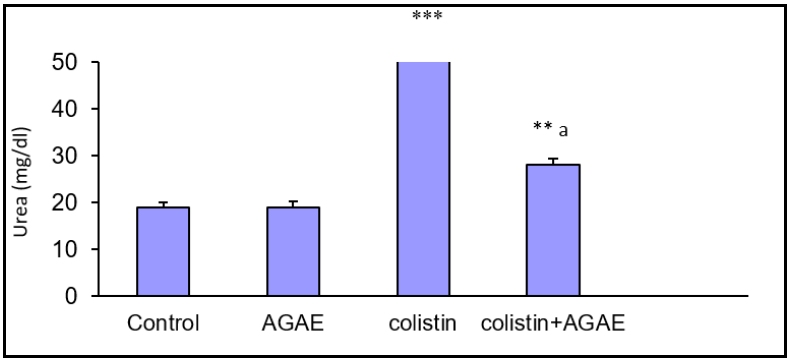

Fig. 12: Effect of different treatments on blood urea level

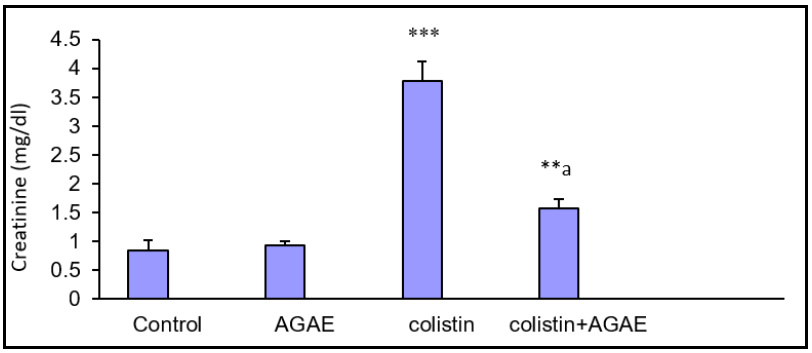

Fig. 13: Effect of different treatments on blood creatinine level.
n= 8 animals in each group
(***): highly significant at $P< 0.0001$ comparing with the control group.
(**): significant at $P<0.0001$ comparing with the control group.
(a): highly significant at $P\leq 0.005$ comparing with colistin group.

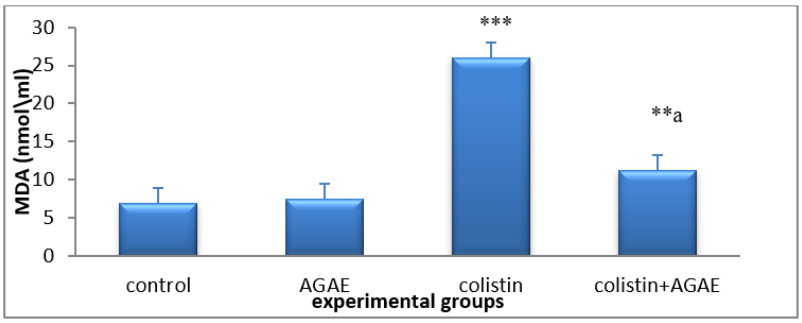

Fig. 14: Effect of different treatments on MDA level

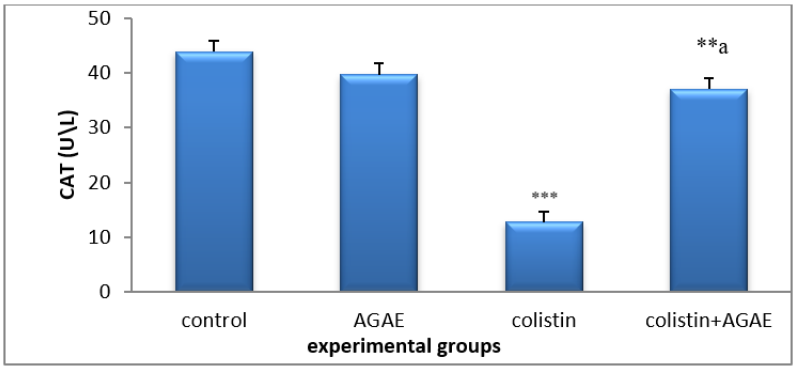

Fig. 15: Effect of different treatments on CAT activity

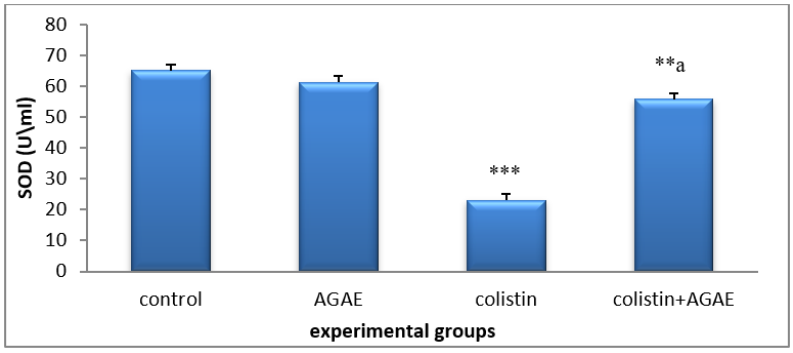

Fig. 16: Effect of different treatments on SOD activity
n= 6 animals in each group
(***): highly significant at $P< 0.0001$ comparing with the control group.
(**): significant at $P<0.001$ comparing with the control group.
(a): highly significant at $P\leq 0.005$ comparing with colistin group.

DISCUSSION

In the present study the treatment with colistin, 84 mg/kg, cumulative dose, showed severe pathological changes in the adrenal cortex include Bowman's capsules, glomeruli, and severe degenerative and necrotic features of tubular epithelium. These changes may be attributed to the oxidative effect of colistin. Similarly, Jeong *et al.,* (2018) reported that colistin treatment resulted in focal tubular degeneration; tubular cells appeared with cytoplasmic vacuolization, blurring brush borders, and shedding epithelial cells. Similarly, Ghlissi *et al.* (2014) reported that colistin treatment caused severe tubular dilation, epithelial vacuolization, and tubular cell necrosis with pyknotic or karyorhexis nuclei with complete loss of chromatin, some cells sloughed within tubular lumen and numerous protein casts were observed. The authors attributed these pathological features to the oxidative stress of colistin and suggested that the primary event in colistin-induced kidney injury is considered the acute proximal tubular damage of necrotic nature.

The rapid renal toxicity of polymyxins is associated with their extensive renal tubular reabsorption, by the proximal tubular cells, that plays a critical role in the extensive accumulation of polymyxins which result in apoptotic cell death by increasing membrane permeability of tubular cells that caused an increase in flex of cation, anions, and water that led to cell swelling, lysis and apoptosis (Azad *et al.,* 2015). Moreover, colistin is poorly diffused across the lipid bilayer membrane and that due to its polycationic nature at physiological *PH* values. Currently, both entrances of colistin inside the cell, endocytic processes, and the facilitation of its transport have been contributed to the colistin uptake through the apical side of proximal tubule cells (Gai *et al.,* 2019).

Concerning the ultrastructural finding in the present work; severe degenerative features of Bowman's capsules, glomeruli, podocyte cells, and the proximal and distal tubular epithelium have appeared. These alternations may be attributed to cellular toxicity and oxidative stress done by colistin. Similarly, Korucu *et al.* (2019) and Samodelov *et al.* (2019) found several ultrastructural features include interstitial edema, epithelial casts in the collecting lumen, dilation of perinuclear cisternae, secondary lysosomes, vacuolization of endothelial cells and the tubular epithelial cells appeared detached from the basement membrane with loss of brush border.

The immunohistochemical observations, the present study showed that the colistin treatment increased the expressions of the apoptotic markers PCNA and Bcl-2. As well, the major signs of apoptosis include mitochondrial Bcl-2 and Bax and endoplasmic reticulum stress was observed in mice upon colistin exposure (Dai *et al.,* 2014). Moreover, marked mitochondrial damage and the elevation of the activity of pro-apoptotic enzyme as caspase-3 was observed in cerebellar cortex of colistin treated mice (Dai *et al*., 2017). Dai *et al.* (2020) reported that colistin treatment up-regulates the activity of Bcl-2 and their mRNA expression as well as increases Bax-mRNA in sciatic nerve of treated animals. Goumenos *et al. (*2009) found high Bcl-2 and Bax expression in the renal tissue of patient with glomerulonephritis and suggested a possible implication of Bcl-2 and Bax in the apoptotic process during the evolution of the human renal disease.

The oxidative stress in the present study recorded an increase in the MDA level and decreases in the activity of SOD in colistin-treated

animals that supports its toxicity, which proved through pathological and ultrastructural changes. Similarly, Ghlissi *et al.* (2014) recorded the same results and suggested that colistin treatment augments reactive oxygen species (ROS) production and renal oxidative stress mediates cell membrane damage and lead to cellular apoptosis, this oxidative stress may be the main mechanism of the nephrotoxicity of colistin (Ozkan *et al.*, 2013; Lee *et al.*, 2015). Our results come in agreement with Ceylan *et al.* (2018) who suggested that the oxidative stress of colistin would be the consequence of excessive production of free radical and the exhaustion of antioxidant enzymes as SOD and CAT causing nephrotoxicity. In addition, ROS targets the mitochondria caused mitochondrial dysfunction and result in cell death by triggering endogenous apoptotic cascade reaction ultimately leading to renal dysfinction (Dai *et al.*, 2016). Colistin can induce rapid cell death through the induction of ROS that leads to oxidative damage of DNA and lipid (Yu *et al.*, 2017).

Examination of sera of animals treated with colistin recorded a significant increase in the level of urea and creatinine that parallel to pathological and ultrastrctural alternations and that may be due to the oxidative stress of colistine that damage the structure of renal cortex tissue and that kidney become dysfunction. Similarly, Talih *et al.* (2018) recorded a significant increase in the values of urea and creatinin in animals treated with colistin. Moreover, nephrotoxicity is associated with colistin therapy because this drug is excreted through the kidney and its elevated blood level may impair kidney function (Ghlissi *et al.*, 2014).

Animals treated only with AGAE showed no pathological, ultrastructural, immunohistochemical, and biochemical changes that indicate the safety of administered of AGAE. These results confirmed previously by Saad *et al.* (2018) who found that normal rat treated with AG did not cause any harm to renal tissue architecture.

The present study reported that treatment with AGAE revealed an advanced degree of improvement in renal pathological, ultrastructural, immunohistochemical and biochemical changes induced by colistin attributed that to the ameliorative effect of AG due to its antioxidant, anti-inflammatory and anti-apoptotic constituents. Similarly, Ali *et al.* (2013) found similar results and suggested that AG exerts both anti-inflammatory and antioxidant action that may counteract the generation of free radical and inflammation associated with chronic induced kidney diseases.

The results of this study illustrated that ultrastructural examination of renal cortex obtained from animals treated with AGAE showed an obvious degree of improvement. The Bowman's capsules, glomeruli and tubular epithelial cells appeared mostly normal. Similarly, Mahmoud *et al.* (2011) reported that electron microscopic examination of damage renal tubules showed an improvement of tubular epithelial cells after AG treatment and confirmed that AG had a protective action against induced nephrotoxicity. Moreover, Gamal El-din *et al.* (2003) found that AG has an anti-inflammatory effect and is used for the treatment of inflammation of intestinal mucosa. Additionally, Nasir *et al.* (2012) revealed that AG treatment delayed the progression to renal failure in diabetic mice. Similar results were obtained by Al Majed *et al.* (2002) who found that co-treated with AG, with different drugs, improved renal tubular cells vacuolization and necrosis and decrease kidney tissue lipid peroxidation indicating possible antioxidant effects. Almohaimeed *et al.* (2019) found that AG treatment

improves the ultrastructural alternations of the sciatic nerve in diabetic animals.

In parallel to the pathological and ultrastructural observations that appeared in the present study the treatment with AGAE led to a nearly normal immunohistochemical expression of both PCNA and Bcl-2 indicating anti-apoptotic activity of AGAE. Similarly**,** Pal *et al.* (2013) suggested that AG could protect the body from ROS effect through two defense mechanisms, primary by antioxidant activity that capable of catalytically removing ROS and the second mechanism by free radical scavengers. Helal *et al.* (2011) observed that AG treatment led to mild PCNA expression in gastric gland.

Concerning the biochemical analysis in the present study revealed that the treatment with AGAE decreases the concentrations of urea and creatinine to normal rang. Moreover, a decrease in the level of elevated MDA and increases in the activities of SOD and CAT were observed. Similarly, Rawoof *et al*. (2017) found that treatment with AG prevents the elevation of serum levels of urea and creatinine. As well, adenine feeding rats that treated with Arabic gum recorded a significant dramatic reduction in serum concentrations of urea and creatinine and uric acid indicating a high improvement in renal function and attributed that to AG ability to reduce uric acid level and other purine metabolites (Saad *et al.,* 2018).

Arabic gum exerts anti-inflammatory and antioxidant effects that may counteract both free radical generation and inflammation-induced chronic kidney disease. Moreover, the induced apoptosis was totally suppressed by Arabic gum in rats suffering from chronic renal failure (Ali *et al.*, 2013). The protective effect of AG may be due to antioxidant activity which is supported by a reduction in lipid peroxidation and elevation of renal SOD (Mahmoud *et al.*, 2011).

Conclusion: it can be concluded that the AGAE exerts a protective effect against renal toxicity through its anti-inflammatory, anti-apoptotic and antioxidant actions.

REFERENCES

Abd-Allah, A.; Al- Yahya, A.; Al-Majed, A.; Gado, A.; Daba, M.; Al-Shabanah, O. and El-Azab A. (2009). *Acacia senegal* gum exudate offers protection against cyclophosphamide induced urinary bladder cytotoxicity. *Oxidative Medicine and Cellular Longevity,* 2: 207-213.

Al Majed, A. A.; Mostafa, A. M.; Al Rikabi, A. C. and Al Shabanah, O. A. (2002). Protective effects of oral Arabic gum administration on gentamicin-induced nephrotoxicity in rats. *Pharmacological Research,* 46: 445-451.

AL Suleimani, Y. M.; AL Zaabi, M.; Ramkumar, A.; AL Mahruqi, A.S.; Tageldin, M. H.;Nemmar,A. Ali, B.H. (2015). Influence of treatment with gum acacia on renal vascular responses in a rat model of chronic kidney disease. *European Review for Medical and Pharmacological Sciences;* 19: 498-509.

Ali, B. H.; Al-Husseni, I.; Beegam, S.; Al-Shukaili, A.; Nemmar, A.; Schierling, S.; Queisser, N. and Schupp, N. (2013). Effect of gum Arabic on oxidative stress and inflammation in adenine-induced chronic renal failure in rats. *PLoS One*, 2013;8: e55242

Almohaimeed, H. M.; Amin, H. A.; Abd El-Aziz, S. A. and Saleh, H. A. (2019). Arabic gum Acacia in combination with

metformin and vitamin B12 improves diabetic peripheral neuropathy in rats: ultrastructural histopathological study. *Journal of Interdisciplinary Histopathology,* 7 (1): 1-9.

Azad, M. A.; Akter, J.; Rogers, K. L.; Nation, R. L.; Velkov, T. and Li, J. (2015). Major pathways of polymyxin-induced apoptosis in rat kidney proximal tubular cells. *Antimicrob Agents Chemother,* 59:2136-2143.

Ceylan, B.; Ozansoy, M.; Kılıç, U.; Yozgat, Y.; Ercan, C, Yıldız, P.; and Aslan, A. (2018). N-acetylcysteine suppresses colistimethate sodium-induced nephrotoxicity via activation of SOD2, eNOS, and MMP3 protein expressions. *Renal Failure,* 40(1): 423-434.

Dai, C, Li J, Tang S.; Li, J. and Xiao, X. (2014). Colistin-induced nephrotoxicity in mice involves the mitochondrial, death receptor, and endoplasmic reticulum pathways. *Antimicrob Agents Chemother,* 58: 4075-4085.

Dai, C.; Ciccotosto, G. D.; Cappai, R.; Wang, Y.; Tang, S.; Xiao, X. and Velko, D. (2017). Minocycline attenuates colistin-induced neurotoxicity via suppression of apoptosis, mitochondrial dysfunction and oxidative stress. *J Antimicrob Chemother,* 72: 1635–1645.

Dai, C.; Tang, S.; Velkov, T. and Xiao, X. (2016). Colistin-indiced apoptosis of neuroblastoma-2a cells involves the generation of reactive oxygen species, mitochondria dysfunction and autophagy. *Molecular Neurobiology,* 53(7): 4685-4700.

Dai, C.; Wang, Y.; Sharma, G.; Shen, J.; Velkov, T. and Xiao, X. (2020). Polymyxins-curcumin combination antimicrobial therapy: safety implications and efficacy for infection treatment. *Antioxidants,* 9, 506; doi:10.3390/antiox9060506

Faid, S. (2013). Biological study on the beneficial effects of Arabic gum on biological parameters of hyperglycemic albino rats. *Life Science Journal,* 10:3570-3579.

Gai, Z.; Samodelov, S. L, Kullak-Ublick, G. A. and Visentin, M. (2019). Molecular mechanisms of colistin-induced nephrotoxicity. *Molecules,* 24 (653):1-14.

Gamal El-din, M.; Mostafa, M.; Al-Shabanah, A.; Al-Bekairi, M. and Nagi, N. (2003). Protective effect of Arabic gum against acetaminophen-induced hepatotoxicity in mice. *Pharmacological Research,* 48: 631-365.

Ghlissi, Z.; Hakim, A.; Mnif, H.; Zeghal, K.; Rebai T. and Sahnoun, Z. (2014). Evaluation of the protective effect of vitamins E and C on acute tubular damage induced by colistin in rat model. merican *Journal of Phytomedicine and Clinical Therapeutics,* 3 (1): 43-53.

Goumenos, D. S.; Tsamandas, A. C.; Kalliakmani, P.; Tsakas, S.; Sotsiou, F.; Bonikos, D. S. and Vlachojannis, J. G. (2009). Expression of apoptosis-related proteins Bcl-2 and Bax along with transforming growth factor (TGF-β1) in the kidney of patients with glomerulonephritis. *Renal Failure,* 26 (4): 361-367.

Helal, O., M.; Yousefa, M. M. and Elnaab, M. (2011). Possible

protective effect of gum arabic on experimentally induced gastric ulcer in adult male albino rats: a histological and immunohistochemical study. *The Egyptian Journal of Histology,* 34:546-553.

Hooda, S.; Pal, R.; Bhandari, A. and Singh, J. (2012). Antioxidant potential and free radical scavenging activity by pod extracts of Acacia Senegal. International *Journal of Pharmaceutical, Chemical and Biological Sciences,* 2: 500-506.

Hsu, S. M.; Raine, L. and Fanger, H. (1981). Avidin and biotin in immunohistochemistry. Histochem. *Cytochemistry,* 29: 1349-1353.

Jeong, B. Y; Park, S.; Cho, S.; Yu, S.; Lee, H. Y.; Park, C. G.; Kang, J.; Jung, D.; Park, M. H.; Hwang, W.; Yun, S.; Jung, J. and Yoon, S. (2018). TGF-b-mediated NADPH oxidase 4-dependent oxidative stress promotes colistin-induced acute kidney injury. *Journal of Antimicrobiaj Chemotherapy,* 73: 962-972.

Korucu, B.; Unal, I.; Pekcan, M.; Inkaya, A. C.; Yeter, H.; Cetinkaya, M. A.; Kaymaz, F. F.; Unal, S.; Akova, M. and Erdem, Y. (2019). Ultrastructural evaluation of urine alkalinization versus hydration on colistin-induced nephrotoxicity.*Human & Experimental toxicology,* 38(12):1366-1377

Lee, S. H.; Kim, J. S.; Ravichandran, K.; Gil, H. W.; Song, H. and Hong, S. Y. (2015). P-glycoprotein induction ameliorates colistin induced nephrotoxicity in cultured human proximal tubular cells. *PLoS One,* 10: e0136075.

Lelon, K.; Jumba, O.; Keter, K.; Chemuku, W. and Oduor, O. (2010). Assessment of physical properties of gum Arabic from *Acacia senegal* varieties in Baringo District, Kenya. *African Journal of Plant Science,* 4: 95-98.

Li, J.; Nation, R. L.; Turnidge, D. Milne, R. W.; Coulthard, K.; Rayner, C. R. and Paterson, D. L. (2006). Colistin: the re-emerging antibiotic for multidrug-resistant Gram-negative bacterial infections. *The Lancet Infectious Diseases,* 6: 589-601.

Mahmoud, M. F.; Diaai, A. A. and Ahmed, F. (2011). Evaluation of the efficacy of ginger, Arabic gum, and *Boswellia* in acute and chronic renal failure. *Renal Failure,* 34(1): 73-82.

Miano, T. A.; Lautenbach, E.; Wilson, F. P.; Guo, W.; Borovskiy, Y. and Hennessy, S. (2018). Attributable risk and time course of colistin-associated acute kidney Injury. *Clinical Journal of the American Society of Nephrology,* 13: 542-550.

Nasir, O.; Umbach, A. T.; Rexhepaj, R.; Ackermann, T. F.; Bhandaru, M.; Ebrahim, A.; Artunc, F.; Kempe, D. S.; Puchchakayala , G.; Siraskar, B.; Foller, M.; Saeed, A. and Lang, F. (2012). Effects of gum Arabic *(Acacia senegal)* on renal function in diabetic mice. *Kidney and Blood Pressure Research,* 35:365-372.

Ozkan, G.; Ulusoy, S.; Orem, A.; Alkanat, M.; Mungan, S.; Yulug, E. and Yucesan, F. B. (2013). How does colistin-induced nephropathy develop and can it be treated? *Antimicrob Agents Chemother,* 57: 3463- 3469.

Pal, R.; Hooda, M.; Bhandari, A. and Singh, J. (2013). Antidiabetic activity of *Acacia senegal* pod extract in streptozotocin-induced diabetic rats. *International Journal of Indigenous Medicinal Plants*, 46: 1400-1404.

Phillips, G. O. (1998). Acacia gum (Gum Arabic): a nutritional fibre; metabolism and calorific value. *Journal Food Additives & Contaminants*, 15: 251-264.

Pogue, J. M.; Lee, J.; Marchaim, D.; Yee, V.; Zhao, J. J.; Chopra, T.; Lephart, P. and Kaye, K. S. (2011). Incidence of and risk factors for colistin-associated nephrotoxicity in a large academic health system. *Clinical Infectious Diseases*, 53: 879-884.

Rawoof, K. G.; Khan, S. A. and Khan, G. A. (2017). Antiurolithiatic activity of gum Arabic on ethylene glycol induced urolithiasis in rat. International *Journal of Pharmacy & Pharmaceutical Research*, 11(1): 88-94.

Saad, E. A.; El-Gayar, H. A.; EL-Demerdash, R. S. and Radwan, K. H. (2018). Hepato-toxic risk of gum Arabic during adenine-induced renal toxicity prevention. *Journal of Applied Pharmaceutical Science*, 8(12): 104-111.

Samodelov, S. L.; Visentin, M.; Gai, Z.; Husler, S, and Kullak-Ublick, G. A. (2019). Renal glycosuria as a novel early sign of colistin-induced kidney damage in mice. *Antimicrobial Agents and Chemotherapy*, (63): 12 e01650-19.

Sivanesan, S. S.; Azad, M. A. K.; Schneider, E. K.; Ahmed, M. U.; Huang, J.; Wang, J.; Li, J. and Nation, R. L. (2017): Gelofusine ameliorates colistin-induced nephrotoxicity.*Antimicrobial Agents and Chemotherapy*, 61(12): e00985-17.

Staples, A. and Wong, C. (2010): Risk factors for progression of chronic kidney disease. *Current Opinion in Pediatrics*, 22: 161-169.

Talih, G.; Esmaoglub, A.; Bayram, A.; Yazici, C.; Deniz, K. and Talih, T. (2018). Does dexmedetomidine prevent colistin nephrotoxicity? *Brazilian Journal of Anestesiology*, 68(4):383-387.

Yahav, D.; Farbman, L.; Leibovici, L. and Paul, M. (2012). Colistin: new lessons on an old antibiotic. *Clinical Microbiology and Infection*, 18:18-29.

Yu, Z.; Zhu, Y.; Qin, W.; Yin, J. and Qiu, J. (2017). Oxidative stress induced by polymyxin E is involved in rapid killing of *Paenibacillus polymyxa*. *BioMed Research International*. Volume 2017, doi.org/10.1155/2017/5437139.